Frontiers in Bioscience Landmark

Front. Biosci. (Landmark Ed) **2023**; 28(4): 65
https://doi.org/10.31083/j.fbl2804065

Original Research

Alterations of Fecal Metabolome Associated with BBIBP-CorV Vaccines against the SARS-CoV-2 Virus

Ying Dong[1,†], Yang Shen[2,†], Pan Wang[1], Jie Jiao[1], Mulei Chen[1,*], Jing Li[1,*]

[1]Heart Center & Beijing Key Laboratory of Hypertension, Beijing Chaoyang Hospital, Capital Medical University, 100020 Beijing, China
[2]Department of Nephrology, Beijing Chaoyang Hospital, Capital Medical University, 100020 Beijing, China
*Correspondence: cml68@sina.cn (Mulei Chen); lijing11999@163.com (Jing Li)
[†]These authors contributed equally.

Academic Editor: Hans-Peter Deigner
Submitted: 13 September 2022 Revised: 25 November 2022 Accepted: 7 December 2022 Published: 6 April 2023

Abstract

Background: The SARS-CoV-2 vaccine has been implemented in response to the 2019 Coronavirus Disease (COVID-19) pandemic worldwide. Dysregulation of gut metabolite is associated with COVID-19 patients. However, the effect of vaccination on the gut metabolite remains unknown, and it is critical to investigate the shifts in metabolic profiles following vaccine treatment. **Methods**: In the present study, we conducted a case-control study to assess the fecal metabolic profiles between individuals who received two doses of intramuscular injection of an inactivated SARS-CoV-2 vaccine candidate (BBIBP-CorV) (n = 20), and matched unvaccinated controls (n = 20) using untargeted gas chromatography and time-of-flight mass spectrometry (GC-TOF/MS). **Results**: Significant different metabolic profiles were observed between subjects receiving SARS-CoV-2 virus vaccines and the unvaccinated. Among a total of 243 metabolites from 27 ontology classes identified in the study cohort, 64 metabolic markers and 15 ontology classes were dramatically distinct between vaccinated and unvaccinated individuals. There were 52 enhanced (such as Desaminotyrosine, Phenylalanine) and 12 deficient metabolites (such as Octadecanol, 1-Hexadecanol) in vaccinated individuals. Along with altered metabolic compositions, multiple functional pathways in Small MoleculePathway Database (SMPDB) and Kyoto Encyclopedia of Genes and Genomes (KEGG) varied between groups. Our results indicated that urea cycle; alanine, aspartate, and glutamate metabolism; arginine and proline metabolism; phenylalanine metabolism and tryptophan metabolism were abundant after vaccination. Additionally, correlation analysis showed that intestinal microbiome was related to alteration in metabolite composition and functions. **Conclusions**: The present study indicated the alterations in the gut metabolome after COVID-19 vaccination and the findings provide a valuable resource for in-depth exploration of mechanisms between gut metabolite and SARS-CoV-2 virus vaccines.

Keywords: gut metabolite; COVID-19; SARS-CoV-2; vaccine; BBINP-CorV

1. Introduction

The 2019 coronavirus disease (COVID-19) is a highly infectious which has become a threat to global health [1]. The number of infections and deaths from COVID-19 is rising alarmingly and on 12 September 2022, there are more than 605,912,418 confirmed cases and 6,491,649 deaths worldwide according to World Health Organization (WHO) COVID-19 Dashboard [2]. In face of such a severe epidemic, vaccination is the best way to control the pandemic. BBIBP-CorV, an inactivated vaccine, is from China National Biotec Group Co. and Beijing Institute of Biological Products, whose safety and performance have been assessed by randomized, double-blind, controlled trials among different groups [3–5].

The human intestinal microbiota consists of 10^{14} resident microbes, including bacteria, archae, viruses and fungi [6]. Numerous of studies indicated that human microbiome is considered to be associated with several disorders, such as hypertension [7], type 2 diabetes mellitus [8], and COVID-19 [9,10]. Ren Z *et al.* [11] demonstrated that compared with healthy controls, the oral and fecal microbial diversity of COVID-19 confirmed patients. Meanwhile, butyric acid-producing bacteria were reduced and lipopolysaccharide-producing bacteria were increased in confirmed patients versus healthy controls in oral cavity. Metabolites in the gastrointestinal tract are the products of microbes such as bacteria and fungi [12]. Meanwhile, previous studies have found significant differences in fecal metabolome profiles not only between COVID-19 patients and healthy controls, but also mild and severe patients. Importantly, these patients were discharged from the hospital with only a small fraction of metabolites returning to normal levels [13].

Evidence from clinical and animal studies indicated that composition and functions of intestinal flora is critical in modulating the immune response to vaccines [14,15]. Ng SC *et al.* [16] found that a higher abundance of *B. adolescentis* was observed in CoronaVac (inactivated COVID-19 vaccine) high-responders, which is related to the immune protection of the enriched carbohydrate metabolic pathways. While, to date, whether inactivated SARS-CoV-2 virus vaccines influences the fecal metabolome profiles

has not been determined. Therefore, in present study, adults who have received inactivated vaccine (BBIBP-CorV) to examine molecular alterations in the gut metabolome using untargeted metabolomics based on time-of-flight mass spectrometry (GC-TOF/MS).

2. Methods

2.1 Inclusion and Exclusion Criteria for the Study Cohort

In the current study, 40 healthy adults, aged between 18–59 years old, were enrolled in Beijing Chaoyang Hospital, and 20 of them were vaccinated since 1 January 2021 to 1 April 2021. The inclusion criteria were as follows: healthy adults who have completely received two doses of intramuscular injection of BBIBP-CorV (as the vaccinated group, n = 20) and 20 unvaccinated individuals (as the unvaccinated group, n = 20). The exclusion criteria were that, participants with cancer, previous heart failure, renal failure, stroke, peripheral artery disease, and chronic inflammation disorders; with previous SARS-CoV-2 exposure or infection; and those who received statin, aspirin, insulin, metformin, antibiotics, or probiotics treatment within the last two months. This study was performed in accordance with the Helsinki declaration, and was approved by the Medical Ethics Committee from Beijing Chaoyang Hospital. Written informed consent was obtained from all study participants prior to enrollment.

2.2 Stool Sample Collection and Preparation

The fresh middle section of the fecal samples was collected from all the participants. And for participants among the vaccinated group, the samples were harvested within 1 month of the second dose of vaccine. All the stool samples were transported to the laboratory and frozen at –80 °C until use. The sample preparation procedures were performed according to the previously published methods [17,18]. Briefly, 5 mg of samples were weighted and placed in a microcentrifuge tube, mixed with 25 mg of prechilled zirconium oxide beads and 10 μL of internal standard. Each aliquot for 50 μL of 50% prechilled methanol (FairLawn, NJ, USA) were applied for automated homogenization. After centrifugation at 14,000 g and 4 °C for 20 min, each aliquot of 175 μL of pre-chilled methanol/chloroform ((FairLawn, NJ, USA)) was added for the extraction. All the samples were evaporated to remove chloroform and lyophilized with a freeze dryer equipped with a stopping tray dryer. The dried sample was derivatized at 30 °C for 2 hour with methoxyamine (St. Louis, MO, USA), and 50 μL of *N*-methyl-*N*-trimethylsilyl-trifluoroacetamide (MSTFA, FairLawn, NJ, USA) was added at 37.5 °C for 1 hour. After derivatization, the samples were injected by a robotic multipurpose sample MPS2 with dual heads.

2.3 Untargeted Metabolomics Based on Time-of-Flight Mass Spectrometry (GC-TOF/MS)

The untargeted metabolomics profiling was performed on XploreMET platform, a GC-TOF/MS system (7890B, Pegasus HT, Leco Corp., St. Joseph, MO, USA) with an Agilent 7890B gas chromatography and a Gerstel multipurpose sample MPS2 (Gerstel, Muehlheim, Germany). A Rxi-5 ms capillary column (30 m $\times$ 250 μm i.d., 0.25-μm film thickness; Restek corporation, Bellefonte, PA, USA) was used for separation. Helium (Parker Balston, Lancaster, NY, USA) was used as the carrier gas at a constant flow rate of 1.0 mL/min. The temperature of injection and transfer interface were both 270 °C. The source temperature was 220 °C. The measurements were made using electron impact ionization (70 eV) in the full scan mode (m/z 50–500).

2.4 Data Preprocessing and Metabolite Annotation

The raw data generated from GC-TOF/MS were processed with ChromaTOF software for automated baseline denosing, smoothing, peak picking, deconvolution and peak alignment. The identification for compound was carried out by comparing both mass spectrometry (MS) similarity and fatty acid methyl esters (FAMEs) retention index distance with the referenced standards in JiaLib database. Briefly, metabolite was annotated by blasting the retention indices and mass spectral data with the previously generated and known structures (as reference standards) in JiaLib metabolite database, which comprises over 1200 mammalian metabolites and has become one of the most comprehensive metabolite libraries. The platform Imap(1.0, Metabo-Profile, Shanghai, China) was used for subsequent statistical analyses.

2.5 Principal Components Analysis (PCA) and Partial Least Square Discriminant Analysis (PLS-DA)

PCA was known as an unsupervised method for modeling, frequently applied to determine data outliers, clustering, and classification trends prior to knowledge of the sample group. The principal components (PCs) such as principal component 1 (PC1) and principal component 2 (PC2) derived from the data set, were orthogonal to one another and could reflect the reducing levels for the variation in the data set. PLS-DA is a generalized multiple regression modeling method dealing with multiple collinear mass spectral data and classes variables. PLS-DA as a multi-class classifier, is utilized to visualize the distinctions in global metabolic profiles between groups. PLS-DA provided more valuable information beyond PCA. The Orthogonal PLSDA (OPLS-DA) is a modification of PLS method, its algorithm decomposed the raw data set into systemic variations, orthogonal/unrelated information, and residual. Statistical algorithms of PCA, PLS-DA and OPLS-DA were adapted from the statistical analysis software packages in R studio (http://cran.r-project.org/, Version 3.3.3, Auckland,

New Zealand).

2.6 Statistical Analysis

Continuous variables were presented as median with interquartile range, while categorical variables were indicated as numbers and percentages. Wilcoxon rank test and chi-squared tests were applied to determine continuous and categorical variables, respectively. Student's *t*-test or Mann-Whitney Wilcoxon test was applied to examine the significant difference between groups. Z score in heatmaps was calculated by subtracting the mean and dividing the standard deviation. Z-score would be negative when the raw value was below the average level and positive when it was higher than the mean. Volcano plot was used to describe the significantly disparate variables between groups. The analyses were performed with SPSS, Version 22.0 (IBM Corp., Armonk, NY, USA). The p values were two-tailed, and a p value < 0.05 was regarded as statistically significant. False discovery rate (FDR) was corrected p value with the Benjamini and Hochberg method.

3. Results

3.1 General Characteristics of the Vaccinated Individuals and Controls

The current study consisted of 20 healthy controls with no history of SARS-CoV-2 virus vaccines vaccination, and 20 individuals who have completed the two doses intramuscular injection of BBIBP-CorV. The clinical information including primary demographics, physiology, and biochemistry characteristics of the participants have been described in **Supplementary Table 1**. Compared with unvaccinated controls, there was no significant difference detected in the vaccinated subjects, either in clinical parameters of sex, body mass index, systolic and diastolic blood pressure levels, fasting blood glucose, total cholesterol, triglyceride, High-Density Lipoprotein Cholesterol (HDLC), Low-Density Lipoprotein Cholesterol (LDLC), uric acid or White Blood Cell (WBC).

3.2 Distinguished Fecal Metabolic Patterns between Vaccinated and Unvaccinated Participants

According to the untargeted metabolomics data based on GC-TOF/MS, we obtained the fecal metabolic characteristics of BBIBP-CorV vaccinated subjects. Clustering analysis of PCA, PLS-DA and OPLS-DA was performed respectively to identify the separation and classification trends. In the PCA plots, vaccinated individuals were observed to be roughly distinguished from the untreated controls (Fig. 1A). There was dramatic difference in both PC1 and PC2 of the PCA plots, with vaccinated subjects displaying much higher score. The PC1 accounted for 20.5% of the whole variance, and PC2 is responsible for 10% of the variance between groups. Similarly, in the PLS-DA scatterplots, we detected clearer clusters of vaccinated and unvaccinated group, respectively (Fig. 1B). An obvious separation between groups was obtained by PLS-DA, and significant distinctions in component 1 and component 2 were confirmed. For component 1, it could explain 18.6% of the difference between groups, and component 2 accounted for 9.04%. Additionally, prominent disparity between individuals who received BBIBP-CorV and the untreated controls was further validated in OPLS-DA analysis (Fig. 1C).

Considering the distinguished metabolic features in vaccinated participants based on multivariate statistical analyses, we further carried out the metabolite annotation. The detailed metabolic composition was obtained, and the top 15 most abundant classes identified were depicted in Fig. 1D. Here we detected 42 amino acids (accounted for 17.28% of total identified metabolites), 37 carbohydrates (15.23%), 31 fatty acids (12.76%), 27 organic acids (11.11%), 16 lipids (6.58%), 15 nucleotides (6.17%), 10 amines (4.12%), 9 alcohols (3.7%), 8 phenols (3.29%), 7 phenylpropanoids (2.88%), 5 bile acids (2.06%), 5 indoles (2.06%), 5 pyridines (2.06%) and 5 vitamins (2.06%).

In addition, there were a total of 27 metabolic classes identified in the study cohort, and the relative abundance and proportion of fecal metabolite classes in each group and individual samples were shown in Fig. 1E,F. The 25 metabolic classes included amino acids, fatty acids, carbohydrates, amines, organic acids, inorganic oxide, lipids, nucleotides, alcohols, pyridines, phenylpropanoic acids, phenols, piperidine, bile acids, piperidinones, phenylpropanoids, benzenoids, vitamins, pyrrolidones, indoles, benzoic acids, short-chain Fatty Acids (SCFAs), imidazolines, amides, imidazoles. It was interesting that the abundance of amino acids, carbohydrates, organic acids, nucleotides, pyrrolidones, benzoic acids and imidazolines were dramatically distinct between vaccinated and unvaccinated subjects, and most of these classes were augmented in vaccinated group.

3.3 The Discriminatory Metabolites between Vaccinated and Control Groups

The composition and percentage of varied fecal metabolite class in vaccinated participants indicated that, the majority of the altered metabolites was mainly consisted of amino acids (58.46%) and carbohydrates (30.41%) (Fig. 2A). As compared with the untreated controls, there were 26 metabolites within the amino acids class and 20 from the carbohydrates class that are discrepant in vaccinated groups (Fig. 2B). Notably, for the total of 243 identified fecal metabolites in the subjects, we observed 99 features significantly different between groups based on univariate analysis ($p < 0.05$), with 83 strikingly upregulated and 16 suppressed metabolic features in the vaccinated group, including decreased 2-amino-2-methyl-1,3-propandiol, threonine, N-formylglycine, asparagine and arabinose etc., as well as increased 1-hexadecanol, octadecanol, sphingosine and heptadecanoic acid etc. (Fig. 2C).

Next, we further focused on the 64 altered metabolic

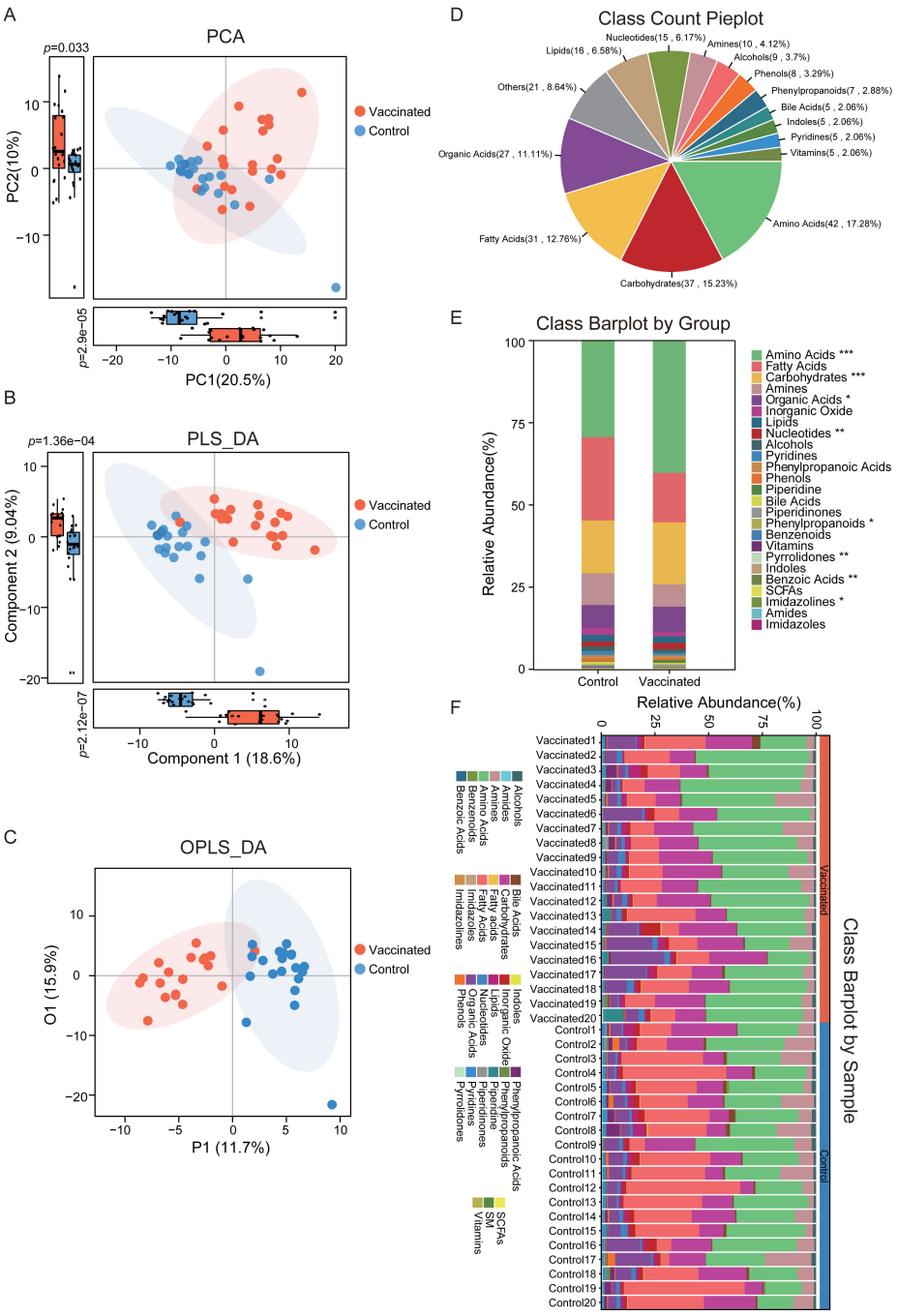

Fig. 1. The discrimination of metabolic profiles between vaccinated and control group. (A) All the samples in vaccinated and control group were distinguished within the PCA plots according to metabolite annotation data. There was bits of overlap between groups, and significant difference was observed in PC1 and PC2, respectively. $p_{c1} = 2.9 \times 10^{-5}$ and $p_{pc2} = 0.033$ between vaccinated and control groups. (B) PLS-DA scatter plots was generated based on the metabolic profiles in stool samples of vaccinated and unvaccinated groups. p values at 1.36×10^{-4} and 2.12×10^{-7} were detected at components 1 and 2, respectively. (C) The scatter plots showed visualization of OPLS-DA for the metabolic profiles in fecal samples from vaccinated and control group. (D) Pie plot showing the proportion of the top15 most abundant metabolic classes identified in the study cohort. (E) All the detected fecal metabolites were classified into 25 classes. The metabolic composition and the relative abundance of each class in vaccinated and unvaccinated groups were indicated in bar plot. Compared with the control group, vaccinated individuals exhibited significantly enriched amino acids, carbohydrates, pyrrolidones, benzoic acids, nucleotides, organic acids, phenylpropanoids and imidazolines. (F) The metabolic composition and the relative abundance of metabolite class in each individuals in vaccinated and control groups. PCA, principal components analysis; PLS-DA, partial least-squares discriminant analysis; OPLS-DA, orthogonal partial least-square discriminant analysis; PC1, principal component 1; PC2, principal component 2.

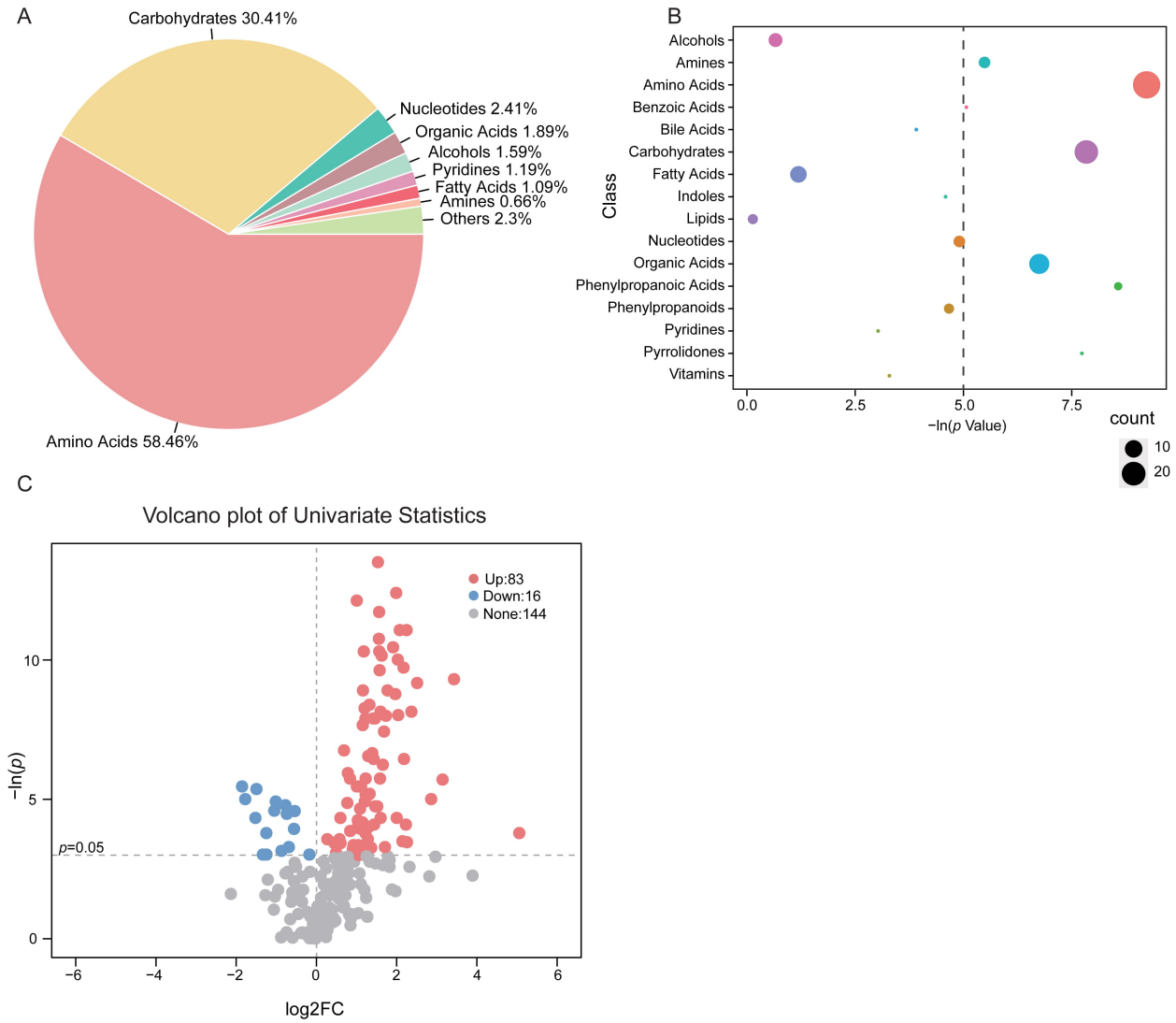

Fig. 2. Shifts of gut metabolic classes in vaccinated subjects. (A) Proportion of the altered metabolite classes in vaccinated group was shown in pie plot. (B) Enrichment of the varied metabolite class in stool samples of vaccinated group. The size of the bubble represented the number of metabolites within the class. The dashed line indicated *p* value at 0.05. (C) Volcano plot depicting the fold change (FC) and *p* value of each identified metabolite. The threshold value for significantly distinct metabolites selection was $p < 0.05$ and $|\log2FC| \geq 0$. In the volcano plot, compared with control subjects, metabolites pointed with red in the right were increased in vaccinated group, and scatters pointed with blue in the left indicated decreased metabolites in vaccinated group.

markers in the stool of vaccinated samples compared with the controls, which showed variable importance in projection (VIP) >1 and significant correlation coefficients (Corr. Coeffs) to component 1 in OPLS-DA. The 64 metabolites were suggested to be with potentials to distinguish vaccinated and control groups. Detailed information such as the class metabolite derived from, HMDB ID, KEGG ID, *p* value, FDR value, fold changes (FC), log2FC, and VIP were described in **Supplementary Table 2**. There were 52 enhanced and 12 deficient metabolites in vaccinated individuals with $p < 0.05$, and Fig. 3A showed their level of *p* value and fold changes. For further investigation, those with significance in the comparison at FDR (corrected *p*) < 0.05 was indicated in Fig. 3B, including octadecanol, 1-hexadecanol, heptadecanoic acid, sphingosine, desaminotyrosine, phenylalanine, 2-hydroxy-3-methylbutyric acid and isoleucine etc.

Relative abundance of the varied fecal metabolites in each vaccinated and unvaccinated individuals were shown in detail with clustering heatmap (Fig. 4A,B). The 9 metabolic markers reduced in vaccinated populations included glycero-3-phosphate, levulinic acid, heptadecanoic acid, 1-hexadecanol, octadecanol, 5beta-coprostanol, phytosphingosine, sphingosine, nonadecanoic acid, which were from lipids, phenylpropanoic acids, organic acids, fatty acids, alcohols, amines and SM, respectively (Fig. 4A). It was interesting that, those enhanced metabolites in stool samples of vaccines-treated partici-

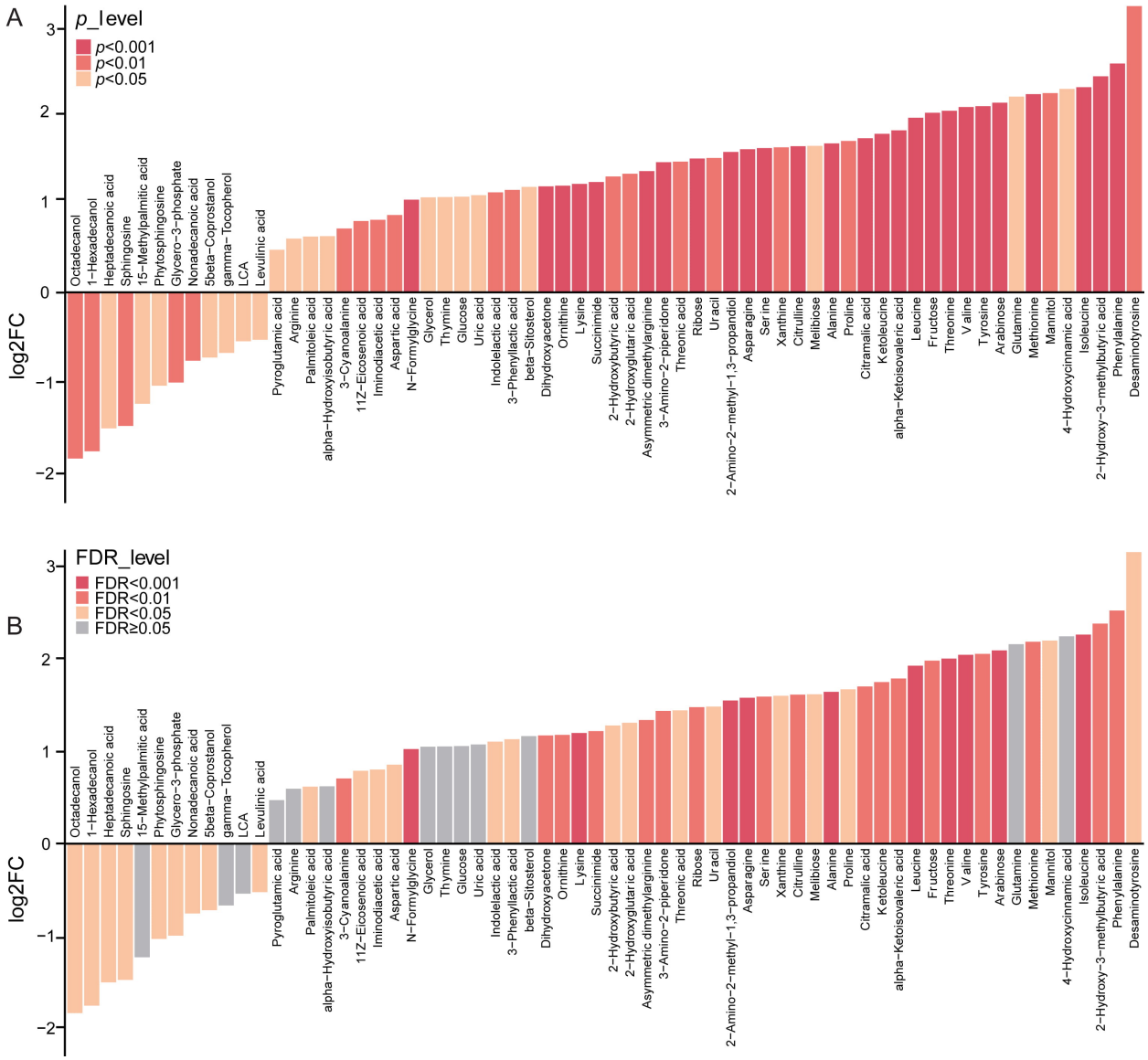

Fig. 3. The alteration of fecal metabolites between vaccinated and un vaccinated group. (A) 64 significantly altered metabolic markers in the stool of vaccinated individuals as compared with the controls, with VIP >1 in multi-dimensional statistics, significant Corr. Coeffs to component 1 in OPLS-DA, $p < 0.05$ and $|\log2FC| \geq 0$ in univariate statistics. Log2FC and bar plot for p values were shown in bar plots. Significance in the comparison was indicated by different colors. Red indicated $p < 0.001$, pink represented $p < 0.01$ and green meant $p < 0.05$. (B) Log2FC and FDR bar plot for the 64 significantly different metabolic markers between vaccinated and unvaccinated individuals. FDR was the false discovery rate, which was obtained through the correction of p value. Red meant FDR <0.001, pink indicated FDR <0.01, green was FDR <0.05, and gray represented FDR ≥0.05.

pants were primarily from amino acids, carbohydrates and organic acids etc., especially essential amino acid. Among them, we found 3-phenyllactic acid, which could be produced by *Bifidobacterium* species via aromatic lactate dehydrogenase, has been previously suggested as contributor to the antiobesity function of green tea polyphenols [19,20].

3.4 Alterations of Metabolic Functional Pathways in Recipients of Vaccines

Next step, we examined the potentials of metabolic and functional pathways in the gut of vaccinated subjects via Small MoleculePathway Database (SMPDB) and Kyoto Encyclopedia of Genes and Genomes (KEGG). The varied fecal metabolite mainly functioned in the process of urea cycle, ammonia recycling, metabolism of aspartate, glycine, serine, arginine, proline, glutathione, galactose, glycerolipid, phenylacetate, phenylalanine and tyrosine, degradation of valine, leucine, isoleucine and homocysteine, biosynthesis of spermidine, spermine and plasmalogen, as indicated by SMPDB (Fig. 5A). The potential metabolic capacities were further confirmed through KEGG pathway analysis, and functions in valine, leucine,

Fig. 4. The distribution of fecal metabolites with significant difference between vaccinated and control group. (A) Heatmap for the significantly shifted metabolites in feces samples of individuals receiving vaccines. The abundance of each metabolite was normalized into Z score. The class of each metabolite was shown in the right of the heatmap. (B) Z-Score plot of varied metabolic biomarkers between groups. The z-score value of 9 metabolites (phytosphingosine, sphingosine, octadecanol, 1-hexadecanol, heptadecanoic acid, glycero-3-phosphate, nonadecanoic acid, 5 beta-coprostanol, levulinic acid) was abundant in the control group, and the z-score of 42 metabolites was enriched in the vaccinated group.

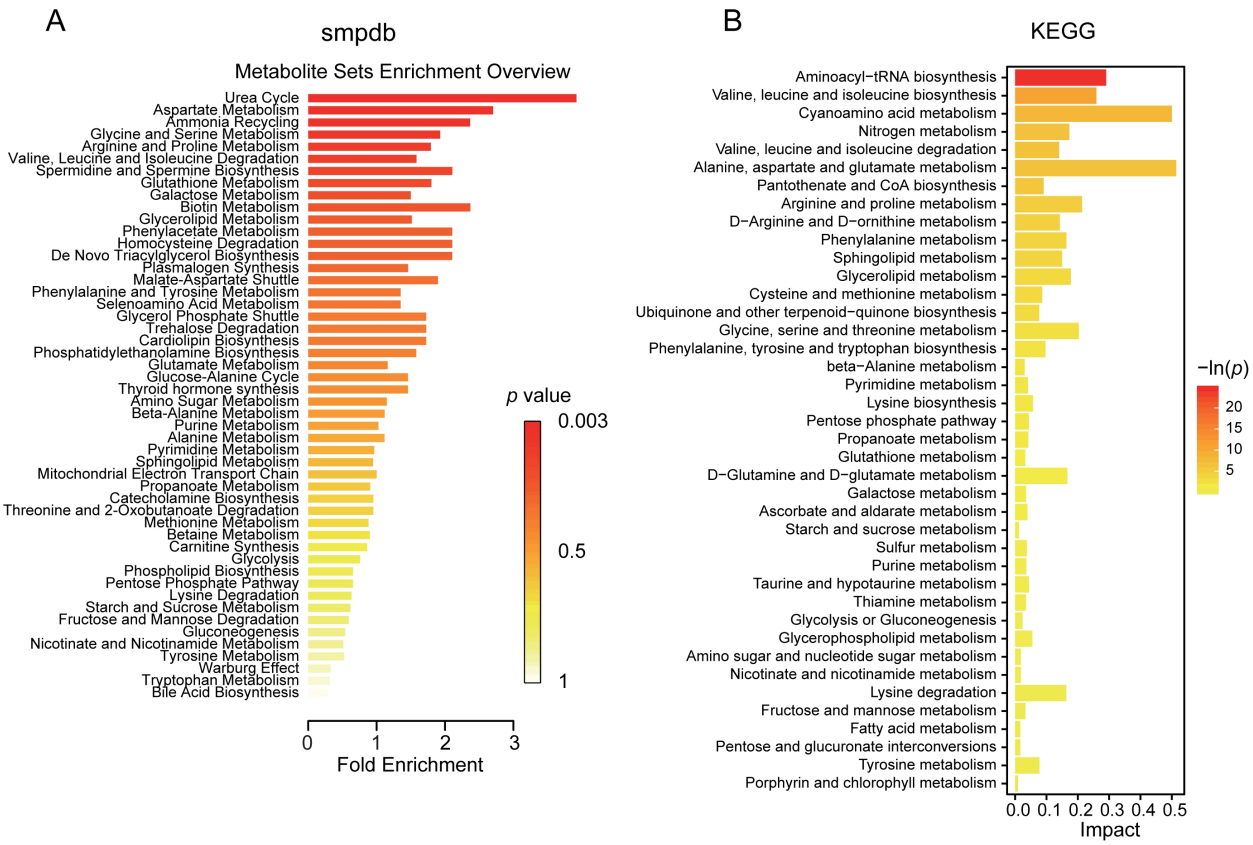

Fig. 5. Potential functional metabolic pathways of the altered metabolites between vaccinated and control group. (A) Pathway enrichment analysis and bar plot based on all the altered metabolites was performed using pathway-associated metabolite sets SMPDB. (B) The KEGG pathway terms identified according to the varied metabolites in the vaccinated group were described in the bar plot. KEGG, Kyoto Encyclopedia of Genes and Genomes; SMPDB, Small Molecule Pathway Database.

isoleucine and lysine degradation, alanine, aspartate, glutamate, arginine, proline and tyrosine metabolism, pentose phosphate pathway were validated (Fig. 5B). These observations demonstrated striking alteration of metabolism in subjects with vaccination.

3.5 Dramatic Correlations of Fecal Metabolome, Intestinal Microbiota and Clinical Characteristics

The significant correlations between different metabolic compositions were determined, and Fig. 6A described the positive or negative relationship of each metabolites. Extremely apparent relevance was detected in the majority metabolites with each other, suggesting the shifts by vaccines treatment might be collaborative. The co-occurrence network of all the varied fecal metabolites with Spearman's correlation coefficients higher than 0.8 was further identified, and all the association were positive (Fig. 6B). For instance, 2-hydroxy-3-methylbutyric acid was positively linked to isoleucine, leucine, phenylalanine, alanine, succinimide and so on; and 4-hydroxycinnamic acid was positively associated with phenylalanine, leucine and isoleucine.

As many fecal metabolites have been indicated to provide functional readout of intestinal microbiome, we thus performed Spearman's correlation analysis between the altered metabolites identified in the present work, and the varied gut microbiota. Here, it was found that, most of the metabolites were negatively related with the microbial taxonomic compositions, except for octadecanol and nonadecanoic acid, *TM7* and *TM7-3* (Fig. 7A). Again, the co-occurrence profiles of fecal metabolome and gut microbiome, with correlation coefficients higher than 0.6, were further indicated in Fig. 7B. *Odoribacteraceae* was identified to be negatively associated with desaminotyrosine, and *Lactococcus* was negatively linked to asparagine. Moreover, almost all the altered fecal metabolites were negatively related to host levels of triglyceride (TG), white blood cell (WBC) and systolic blood pressure (SBP), but positively to low-density lipoprotein cholesterol (LDL) (Fig. 8A). Also here, obvious correlations was identified, including positive association between desaminotyrosine and uric acid (UC), negative relationship between WBC and 2-Amino-2-methyl-1,3-propandiol, Isoleucine, Leucine, Methionine and Ribose, respectively. Ribose was observed to be negatively related with TG levels (Fig. 8B, correlation coefficients >0.5).

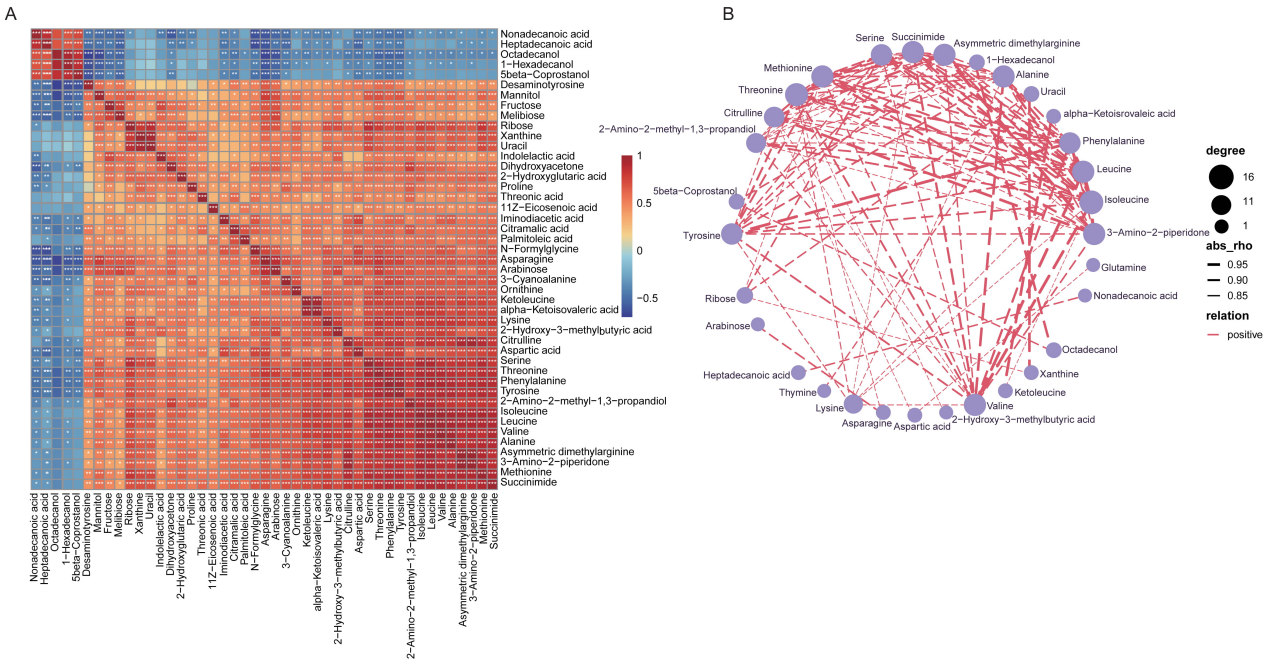

Fig. 6. Spearman's correlation of the top 50 most dominant fecal metabolites shifted in vaccinated individuals and the network relationship. (A) Heatmap showing Spearman's correlation analysis for the co-occurrence profiles of the top 50 most correlated fecal metabolites altered between groups. The correlation coefficient was expressed in different colors. Red, positive correlation; Blue, negative correlation. *, $p < 0.05$; **, $p < 0.01$; ***, $p < 0.001$. (B) Correlation network for the top 50 most enriched fecal metabolites, which varied significantly between groups and showed coefficient >0.8 to each other. Positive correlation between nodes was indicated by red connecting lines. Spearman's correlation, $p < 0.05$ and absolute coefficient >0.8. Degree indicated the number of other nodes that each node was connected to.

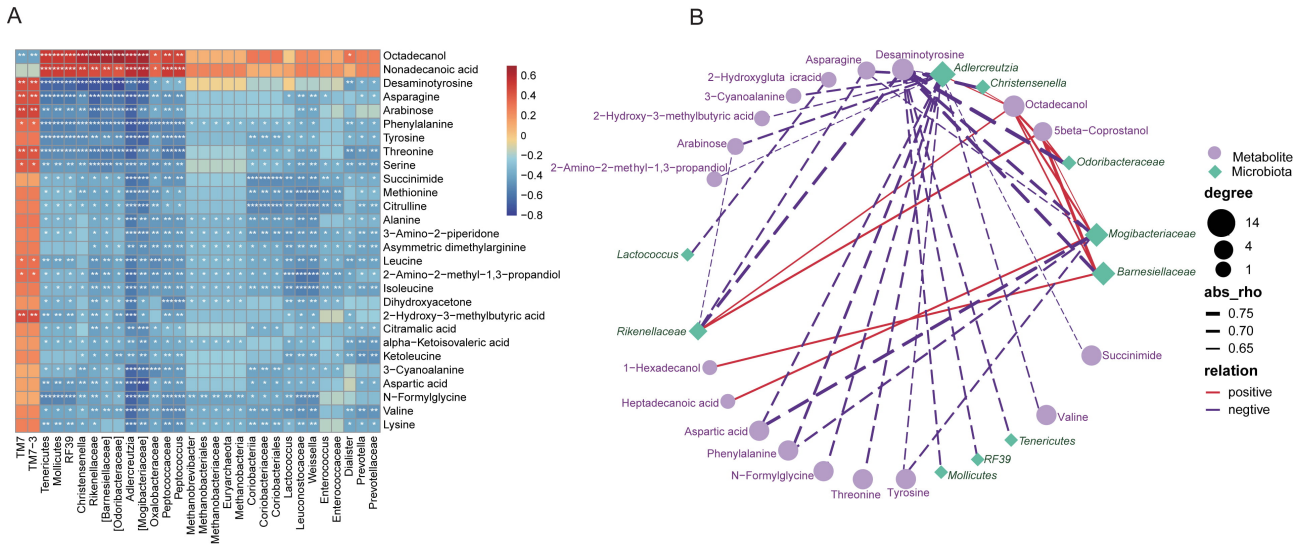

Fig. 7. Vaccines-associated fecal metabolites correlated with the gut microbiota differentiated in vaccinated individuals. (A) Heatmap describing Spearman's correlation for the association between the top 30 altered metabolites and the top 30 most correlated gut microflora shifted in vaccinated subjects. The correlation coefficient was expressed in colors. Red, positive correlation; Blue, negative correlation. *, $p < 0.05$; **, $p < 0.01$; ***, $p < 0.001$. (B) Correlation network of the most striking shifted metabolites and disordered gut microflora between groups, with coefficient >0.6 to each other. Purple circles indicated metabolites, and green diamond indicated gut microflora. Spearman's correlation, $p < 0.05$ and absolute coefficient >0.6. Positive correlation between nodes was indicated by red connecting lines, and negative correlation was by blue lines. Degree indicated the number of other nodes that each node was connected to.

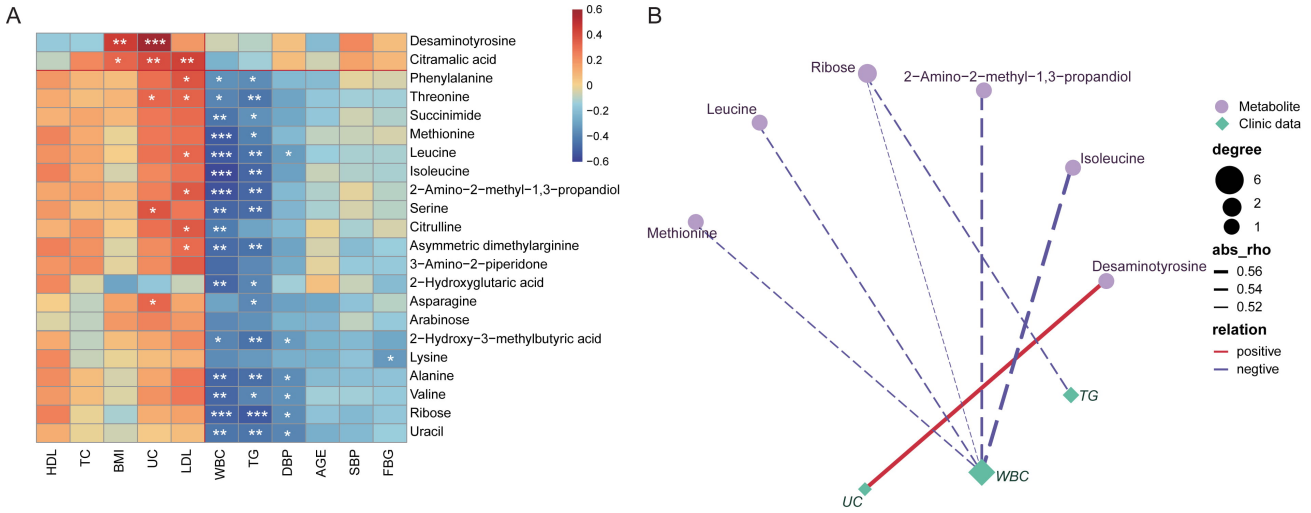

Fig. 8. Correlation analysis between the altered fecal metabolites and clinical characteristics of the study cohort. (A) Spearman's correlation analysis of the association between the varied metabolites (most correlated 22 metabolites) and the clinical characteristics of each participants. The correlation coefficient was expressed in colors. Red, positive correlation; Blue, negative correlation. *, $p < 0.05$; **, $p < 0.01$; ***, $p < 0.001$. (B) Co-abundance network for the correlation between the fecal metabolites and the clinical characteristics. Purple circles denoted metabolites, and green diamond indicated clinical characteristics. Spearman's correlation, $p < 0.05$ and absolute coefficient >0.5 between metabolite and clinical characteristics. Positive correlation between nodes was indicated by red connecting lines, and negative correlation by blue. Degree indicated the number of other nodes that each node was connected to. HDL, high-density lipoprotein cholesterol; TC, total cholesterol; BMI, body mass index; UC, uric acid; LDL, low-density lipoprotein cholesterol; WBC, white blood cell; TG, triglyceride; DBP, diastolic blood pressure; SBP, systolic blood pressure; FBG, fasting blood glucose.

4. Discussion

In the present study, we observed that the fecal metabolome profiles were disparate significantly between subjects receiving SARS-CoV-2 virus vaccines and those unvaccinated. Among a total of 243 metabolites from 27 ontology classes identified in the study, 64 metabolic markers and 15 ontology classes were dramatically distinct between vaccinated and unvaccinated individuals. There were 52 enhanced such as Desaminotyrosine, Phenylalanine, and 12 deficient metabolites such as Octadecanol, 1-Hexadecanol in the vaccinated individuals. Furthermore, correlation analysis indicated that intestinal microbiome was related to alterations in metabolite composition and functions.

Currently, BBIBP-CorV has received emergency use from the WHO, meanwhile it is approved for use in more than 45 countries worldwide [21]. In China, BBIBP-CorV, as one of the major inactivated COVID-19 vaccines, has been shown to be generally safe and elicit effective antibody responses [22,23]. As of now, accumulating evidence show that the gut microbiome plays an essential role in the progression of COVID-19 [10,24]. Yeoh YK *et al.* [9] found that the gut microbiome of COVID-19 patients was strongly disturbed compared with healthy controls, with depletion of beneficial commensal bacteria including *Faecalibacterium prausnitzii*, *Eubacterium rectale* and enrichment of conditional pathogenic bacteria such as *Clostridium hathewayi*, *Bacteroides nordii* in the gastrointestinal tract. Most recently, investigators indicated that gut microbiome ecology was stratified well with COVID-19 severity. With availability of COVID-19 vaccines, researchers have identified the alterations in oral and intestinal microbiomes of vaccinated individuals [16,25]. However, the effect of BBIBP-CorV vaccination on metabolites thought to be downstream of gut microbiota has not been determined. Here we for the first time explored the shifts of gut metabolites after vaccination.

Overall, the metabolite profiles of gut microbiota in vaccinated individuals were significantly different from those within unvaccinated subjects. Specifically, we found that the expression levels of several metabolites, such as desaminotyrosine, glutamine, isoleucine, were prominently abundant in vaccine recipients. Previous study showed that desaminotyrosine could elicit protection against the influenza virus [26]. Desaminotyrosine was further confirmed by Steed *et al.* [27] to suppress influenza and reduce lung immunopathology. In addition, glutamine is an L-α gluconeogenic and proteogenic amino acid containing five carbons and two amino groups [28]. Glutamine exerts an antiinflammatory activity and prevents the expression of pro-inflammatory cytokines by the inhibition of both nuclear factor *k* light chain-enhancer of activated B cells and signal transducer and activator of transcription proteins [29]. Currently, glutamine is thought to be the fuel for the immune system, generating the concept of immunometabolism [30]. Meanwhile, plasma levels of

glutamine were markedly deficient among inflammatory bowel disease patients, especially during the acute exacerbation of Crohn's disease [31,32]. Moreover, compared to that before the onset of COVID-19, a 19% reduction in glutamine blood level was observed in patients following infection [33]. While in our study, it was found that the abundance of desaminotyrosine and glutamine were both enhanced compared with unvaccinated subjects, which indicated that vaccine might play a potential role in resisting from SARS-CoV-2 virus after injection.

In addition, in the present work, we have identified that several metabolites were depressed in the gut of vaccinated individuals in comparison with unvaccinated subjects, especially for Heptadecanoic acid etc. Heptadecanoic acid as a kind of odd chain saturated fatty acids, has been known to play an essential role in various important biological and nutritional process [34]. The EPIC-Norfolk prospective study showed that Heptadecanoic acid abundance was negatively associated with coronary heart disease risk [35]. Furthermore, recent observation based on the EPIC and INTERACT studies indicated that Heptadecanoic acid also exhibited a strong inverse correlation with type II diabetes [36]. Based on our findings of suppressed Heptadecanoic acid after SARS-CoV-2 vaccination, it was speculated that the reduction of protective Heptadecanoic acid in response to vaccines might be related to some typical side effects of BBIBP-CorV vaccines.

Previously, study has compared the serum metabolic profiles of pre-vaccination samples with post-vaccination samples from the same individual upon Sinovac COVID-19 vaccines but not BBIBP-CorV vaccines [37]. He M and colleagues [37] examined sera samples from 30 individuals before SARS-CoV-2 vaccination (Sinovac) and 29 thereinto after two-dose vaccination. Under untargeted liquid chromatography-mass spectrometry/mass spectrometry analysis, several metabolites such as L-glutamic acid, gamma-aminobutyric acid, succinic acid, and taurine showed increasing shifts from post-vaccination to pre-vaccination. Moreover, metabolites associated with two-dose vaccination mainly participated in butanoate metabolism and glutamate metabolism. Whereas there remains limited knowledge of alterations in fecal metabolome before and after BBIBP-CorV vaccination, and further attempts to clarify this should be a priority in future studies.

Along with altered metabolic compositions, multiple functional pathways in SMPDB and KEGG were detected to be varied dramatically between groups. Our results indicated that urea cycle; alanine, aspartate, and glutamate metabolism; arginine and proline metabolism; phenylalanine metabolism and tryptophan metabolism were more enriched after vaccination. The urea cycle (ornithine cycle) is a critical amino acid metabolism pathway for waste nitrogen dispose in mammals [38]. Previous studies showed that urea cycle dysregulation plays a crucial role in regulating various metabolic processes, leading to hyperornithinemia, hyperammonemia and gyrate atrophy in humans [39]. Besides, urea cycle dysfunction serves as a biofluids biomarker in cancer patients and is implicated inenhanced response to immune checkpoint therapy [40]. It was quite interesting that, Li T *et al*. [41] found that among severe COVID-19 patients, the urea cycle is also significantly aberrant. Even in the early stages of severe COVD-19, patients also exhibited abnormal profiles in three amino acid pathways including alanine, aspartate, and glutamate metabolism; arginine and proline metabolism; phenylalanine metabolism. However, when compared with unvaccinated controls, vaccinated subjects showed enrichment in these amino acid pathways mentioned above. The possible reason for this phenomenon might be that the inactivated vaccines enable the adaptive immune system to form a lasting memory of viral component [42], which in turn enabled vaccinated subjects less susceptible to SARS-CoV-2 invasion and more resistant to COVID-19.

As previously reported, carbohydrate and amino acid metabolism are essential for immune cells to survive, proliferate and function [42]. Our results indicated that fructose and arabinose of the carbohydrates was positively correlated with serine and succinimide within the amino acids. Fructose is indicated to be an important cause of obesity and obesity-related cardiometabolic complications [43,44]. Evidence suggested that fructose-induced obesity showed higher level of chronic inflammation, and accumulation of macrophages in adipose tissues, which are responsible for the production of TNF-α, IL-6, NO, and IL-1β [45,46]. In addition, important epigenetic role for serine has been uncovered in a number of immune cells [47]. In T cells, serine was crucial to proliferation by supporting purine biosynthesis [48]. Moreover, immune cells can acquire serine through de novo synthesis or extracellular uptake [49]. Collectively, to a certain extent, the positive correlation between carbohydrate (fructose etc.) and amino acids (serine etc.) might be closely related to immune responses of SARS-CoV-2 vaccines.

In the present study, it was found that the majority altered fecal metabolites were negatively related to intestinal microbiota. *Enterococcus* is an important opportunistic pathogen causing a wide variety of infections [50], which is extremely enriched in various diseases such as coronary artery disease [51] and infective endocarditis [52]. Previous study has detected negative correlation between *Enterococcus* and isoleucine, and total amino acids in animal models [53]. We also found that *Enterococcus* was negatively linked with several essential amino acid metabolites that were elevated in the vaccinated group, such as Isoleucine, Leucine and Methionine. It was speculated that upon COVID-19 vaccines, shifts of intestinal flora might directly or indirectly affect the profiles of metabolites and thus play a role in immune regulation.

Branched-chain amino acids including Leucine, Isoleucine and Valine, exert a vital role in modulating

body weight and muscle protein synthesis [54]. Ma Q *et al*. [55] suggested that Leucine, Isoleucine or their combination in drinking water significantly decreased relative white adipose tissue weight, serum TG and free fatty acid compared with mice fed with high fat diet. These observations are in line with our findings of the negative relationship between TG and Leucine, Isoleucine, Valine, respectively. Furthermore, previous study indicated that desaminotyrosine exhibited obvious toxicities to the kidney at a higher dose [56]. Oral administration of high-dose desaminotyrosine significantly affected the renal function indexes by elevating blood urea nitrogen and creatinine in animals. Moreover, histopathological analysis uncovered severe granules and vacuolar degeneration of renal tubular epithelial cells and interstitial edema in response to desaminotyrosine [56]. It is well known that enhanced level of UC is important risk factor for kidney disease [57,58]. Here we demonstrate a positive correlation between UC and desaminotyrosine, the causality of which requires further confirmation.

In current study, we found that COVID-19 vaccines elicited alterations in multiple metabolites, which exerted potential roles in differential functional pathways, and might further correlated with blood antibody and cytokine response. The varied fecal metabolites were revealed to mainly function in the processes of amino acid metabolism. For example, succinic acid semialdehyde, L-glutamic acid, Gamma-Aminobutyric acid, succinic acid and oxoglutaric acid were inalanine, aspartate and glutamate metabolism, and L-glutamic acid, oxoglutaric acid were in D-Glutamine and D-glutamate metabolism. It has been documented that inactivated SARS-CoV-2 vaccines could produce rapid and strong antibody responses, such as IgG, making them critical during the pandemic of COVID-19 [5]. Previous evidence suggested that metabolites L-glutamic acid, succinic acid semialdehyde and succinic acid involved in the alanine, aspartate and glutamate metabolism, as well as D-Glutamine and D-glutamate metabolism pathways identified in our study were positively correlated with the levels of IgM, IgG or IgA [37]. This information facilitates us to speculate that the highlighted metabolites and metabolic pathways might be closely related to body's immune responses after immunization.

Understanding how SARS-CoV-2 vaccines affect the composition of metabolites downstream of gut microbiota may provide important information regarding alterations within the gut environment following immune responses to SARS-CoV-2 infection. Nevertheless, there are several limitations in the current study. Firstly, the data interpretation might be limited due to relatively small sample size, and the conclusions need to be validated by larger studies. Additionally, in the present study, samples from a single time point after vaccination were analyzed, and the composition of intestinal metabolites might have varied at different time points after vaccination. Thus, further studies including sampling at different time points after vaccination could provide more reliable information on temporal function due to COVID-19, reveal the effect of COVID-19 vaccination on the metabolic composition of gut mcirobiota, and elucidate the underlying mechanisms.

5. Conclusions

The present study depicted the alterations in the gut metabolome after COVID-19 vaccination based on GC-TOF/MS methods. Our observations support an association between the gut microbiome, metabolite perturbation, and COVID-19 vaccination, and provide valuable resource for in-depth exploration of metababolic profiles in vaccinated individuals, understanding the complex mechanisms between gut metabolite and SARS-CoV-2 virus vaccines.

Availability of Data and Materials

Data sets used and analysed during the current study are available from the corresponding author on reasonable request.

Author Contributions

JL, MC, YD and YS—conceived the study, directed the project, designed the experiments. JL, YD and YS—interpreted the results and wrote the manuscript. PW, JJ, YS, MC—recruited and collected the clinical details from the subjects. JL and YD—analyzed the data. JL, MC, YD and YS—revised the manuscript. All authors contributed to editorial changes in the manuscript. All authors read and approved the final manuscript.

Ethics Approval and Consent to Participate

This study was performed in accordance with the Helsinki declaration, and was approved by the Medical Ethics Committee from Beijing Chaoyang Hospital. Written informed consent was obtained from all study participants prior to enrollment (ethical number: 2021-ke-440).

Acknowledgment

Not applicable.

Funding

This research received no external funding.

Conflict of Interest

The authors declare no conflict of interest.

Supplementary Material

Supplementary material associated with this article can be found, in the online version, at https://doi.org/10.31083/j.fbl2804065.

References

[1] Wang C, Horby PW, Hayden FG, Gao GF. A novel coronavirus outbreak of global health concern.The Lancet. 2020; 395: 470–473.

[2] World Health Organization. WHO Coronavirus (COVID-19) Dashboard. 2022. Available at: https://covid19.who.int/ (Accessed: 12 September 2022).

[3] Guo W, Duan K, Zhang Y, Yuan Z, Zhang Y, Wang Z, *et al*. Safety and immunogenicity of an inactivated SARS-CoV-2 vaccine in healthy adults aged 18 years or older: a randomized, double-blind, placebo-controlled, phase 1/2 trial. EClinicalMedicine. 2021; 38: 101010.

[4] Xia S, Duan K, Zhang Y, Zhao D, Zhang H, Xie Z, *et al*. Effect of an Inactivated Vaccine Against SARS-CoV-2 on Safety and Immunogenicity Outcomes: Interim Analysis of 2 Randomized Clinical Trials. The Journal of the American Medical Association. 2020; 324: 951–960.

[5] Xia S, Zhang Y, Wang Y, Wang H, Yang Y, Gao GF, *et al*. Safety and immunogenicity of an inactivated COVID-19 vaccine, BBIBP-CorV, in people younger than 18 years: a randomised, double-blind, controlled, phase 1/2 trial. The Lancet Infectious Diseases. 2022; 22: 196–208.

[6] Gill SR, Pop M, DeBoy RT, Eckburg PB, Turnbaugh PJ, Samuel BS, *et al*. Metagenomic Analysis of the Human Distal Gut Microbiome. Science. 2006; 312: 1355–1359.

[7] Li J, Zhao F, Wang Y, Chen J, Tao J, Tian G, *et al*. Gut microbiota dysbiosis contributes to the development of hypertension. Microbiome. 2017; 5: 1–19.

[8] Qin J, Li Y, Cai Z, Li S, Zhu J, Zhang F, *et al*. A metagenome-wide association study of gut microbiota in type 2 diabetes. Nature. 2012; 490: 55–60.

[9] Yeoh YK, Zuo T, Lui GC, Zhang F, Liu Q, Li AY, *et al*. Gut microbiota composition reflects disease severity and dysfunctional immune responses in patients with COVID-19. Gut. 2021; 70: 698–706.

[10] Zuo T, Zhang F, Lui GCY, Yeoh YK, Li AYL, Zhan H, *et al*. Alterations in Gut Microbiota of Patients with COVID-19 during Time of Hospitalization. Gastroenterology. 2020; 159: 944–955.e8.

[11] Ren Z, Wang H, Cui G, Lu H, Wang L, Luo H, *et al*. Alterations in the human oral and gut microbiomes and lipidomics in COVID-19. Gut. 2021; 70: 1253–1265.

[12] Noerman S, Kolehmainen M, Hanhineva K. Profiling of Endogenous and Gut Microbial Metabolites to Indicate Metabotype-Specific Dietary Responses: a Systematic Review. Advances in Nutrition. 2020; 11: 1237–1254.

[13] Lv L, Jiang H, Chen Y, Gu S, Xia J, Zhang H, *et al*. The faecal metabolome in COVID-19 patients is altered and associated with clinical features and gut microbes. Analytica Chimica Acta. 2021; 1152: 338267.

[14] Lynn DJ, Benson SC, Lynn MA, Pulendran B. Modulation of immune responses to vaccination by the microbiota: implications and potential mechanisms. Nature Reviews Immunology. 2022; 22: 33–46.

[15] de Jong SE, Olin A, Pulendran B. The Impact of the Microbiome on Immunity to Vaccination in Humans. Cell Host Microbe. 2020; 28: 169–179.

[16] Ng SC, Peng Y, Zhang L, Mok CK, Zhao S, Li A, *et al*. Gut microbiota composition is associated with SARS-CoV-2 vaccine immunogenicity and adverse events. Gut. 2022; 71: 1106–1116.

[17] Qiu Y, Cai G, Su M, Chen T, Zheng X, Xu Y, *et al*. Serum Metabolite Profiling of Human Colorectal Cancer Using GC−TOFMS and UPLC−QTOFMS. Journal of Proteome Research. 2009; 8: 4844–4850.

[18] Wang J, Chen W, Li J, Wu S, Chen T, Zhu Y, *et al*. Prognostic significance of 2-hydroxyglutarate levels in acute myeloid leukemia in China. Proceedings of the National Academy of Sciences. 2013; 110: 17017–17022.

[19] Zhou J, Tang L, Shen C, Wang J. Green tea polyphenols modify gut-microbiota dependent metabolisms of energy, bile constituents and micronutrients in female Sprague–Dawley rats. The Journal of Nutritional Biochemistry. 2018; 61: 68–81.

[20] Laursen MF, Sakanaka M, von Burg N, Morbe U, Andersen D, Moll JM, *et al*. Bifidobacterium species associated with breastfeeding produce aromatic lactic acids in the infant gut. Nature Microbiology. 2021; 6: 1367–1382.

[21] World Health Organization. Evidence Assessment: Sinopharm/BBIBP COVID-19 Vaccine. 2021. Available at: https://cdn.who.int/media/docs/default-source/immunization/sage/2021/april/2_sage29apr2021_critical-evidence_sinopharm.pdf?sfvrsn=3dfe32c1_5 (Accessed: 8 September 2022).

[22] Xia S, Zhang Y, Wang Y, Wang H, Yang Y, Gao GF, *et al*. Safety and immunogenicity of an inactivated SARS-CoV-2 vaccine, BBIBP-CorV: a randomised, double-blind, placebo-controlled, phase 1/2 trial. The Lancet Infectious Diseases. 2021; 21: 39–51.

[23] Al Kaabi N, Zhang Y, Xia S, Yang Y, Al Qahtani MM, Abdulrazzaq N, *et al*. Effect of 2 Inactivated SARS-CoV-2 Vaccines on Symptomatic COVID-19 Infection in Adults: A Randomized Clinical Trial. The Journal of the American Medical Association. 2021; 326: 35–45.

[24] Zuo T, Zhan H, Zhang F, Liu Q, Tso EYK, Lui GCY, *et al*. Alterations in Fecal Fungal Microbiome of Patients with COVID-19 during Time of Hospitalization until Discharge. Gastroenterology. 2020; 159: 1302–1310.

[25] Uehara O, Abiko Y, Nagasawa T, Morikawa T, Hiraki D, Harada F, *et al*. Alterations in the oral microbiome of individuals with a healthy oral environment following COVID-19 vaccination. BMC Oral Health. 2022; 22: 1–9.

[26] Gautier T, David-Le Gall S, Sweidan A, Tamanai-Shacoori Z, Jolivet-Gougeon A, Loréal O, *et al*. Next-Generation Probiotics and Their Metabolites in COVID-19. Microorganisms. 2021; 9: 941.

[27] Steed AL, Christophi GP, Kaiko GE, Sun L, Goodwin VM, Jain U, *et al*. The microbial metabolite desaminotyrosine protects from influenza through type I interferon. Science. 2017; 357: 498–502.

[28] Cortes GM, Marcialis MA, Bardanzellu F, Corrias A, Fanos V, Mussap M. Inflammatory Bowel Disease and COVID-19: How Microbiomics and Metabolomics Depict Two Sides of the Same Coin. Frontiers in Microbiology. 2022; 13: 1–24.

[29] Kretzmann NA, Fillmann H, Mauriz JL, Marroni CA, Marroni N, González-Gallego J, *et al*. Effects of glutamine on proinflammatory gene expression and activation of nuclear factor kappa B and signal transducers and activators of transcription in TNBS-induced colitis. Inflammatory Bowel Diseases. 2008; 14: 1504–1513.

[30] Wang A, Luan HH, Medzhitov R. An evolutionary perspective on immunometabolism. Science. 2019; 363: eaar3932.

[31] Scoville EA, Allaman MM, Brown CT, Motley AK, Horst SN, Williams CS, *et al*. Alterations in lipid, amino acid, and energy metabolism distinguish Crohn's disease from ulcerative colitis and control subjects by serum metabolomic profiling. Metabolomics. 2018; 14: 17.

[32] Sido B, Seel C, Hochlehnert A, Breitkreutz R, Dröge W. Low Intestinal Glutamine Level and Low Glutaminase Activity in Crohn's Disease: a Rational for Glutamine Supplementation? Digestive Diseases and Sciences. 2006; 51: 2170–2179.

[33] Bruzzone C, Bizkarguenaga M, Gil-Redondo R, Diercks T, Arana E, García de Vicuña A, *et al*. SARS-CoV-2 Infection Dysregulates the Metabolomic and Lipidomic Profiles of Serum. iScience. 2020; 23: 101645.

[34] Jenkins B, West JA, Koulman A. A review of odd-chain fatty acid metabolism and the role of pentadecanoic Acid (c15:0) and heptadecanoic Acid (c17:0) in health and disease. Molecules. 2015; 20: 2425–2444.
[35] Khaw KT, Friesen MD, Riboli E, Luben R, Wareham N. Plasma phospholipid fatty acid concentration and incident coronary heart disease in men and women: the EPIC-Norfolk prospective study. PLoS Medicine. 2012; 9: e1001255.
[36] Forouhi NG, Koulman A, Sharp SJ, Imamura F, Kröger J, Schulze MB, *et al*. Differences in the prospective association between individual plasma phospholipid saturated fatty acids and incident type 2 diabetes: the EPIC-InterAct case-cohort study. The Lancet Diabetes and Endocrinology. 2014; 2: 810–818.
[37] He M, Huang Y, Wang Y, Liu J, Han M, Xiao Y, *et al*. Metabolomics-based investigation of SARS-CoV-2 vaccination (Sinovac) reveals an immune-dependent metabolite biomarker. Frontiers in Immunology. 2022; 13: 5741.
[38] Morris SM Jr. Regulation of enzymes of the urea cycle and arginine metabolism. Annual Review of Nutrition. 2002; 22: 87–105.
[39] Sivashanmugam M, Jaidev J, Umashankar V, Sulochana KN. Ornithine and its role in metabolic diseases: an appraisal. Biomedicine and Pharmacotherapy. 2017; 86: 185–194.
[40] Lee JS, Adler L, Karathia H, Carmel N, Rabinovich S, Auslander N, *et al*. Urea Cycle Dysregulation Generates Clinically Relevant Genomic and Biochemical Signatures. Cell. 2018; 174: 1559–1570.
[41] Li T, Ning N, Li B, Luo D, Qin E, Yu W, *et al*. Longitudinal Metabolomics Reveals Ornithine Cycle Dysregulation Correlates With Inflammation and Coagulation in COVID-19 Severe Patients. Frontiters in Microbiology. 2021; 12: 723818.
[42] Madison AA, Shrout MR, Renna ME, Kiecolt-Glaser JK. Psychological and Behavioral Predictors of Vaccine Efficacy: Considerations for COVID-19. Perspectives on Psychological Science. 2021; 16: 191–203.
[43] Taskinen MR, Söderlund S, Bogl LH, Hakkarainen A, Matikainen N, Pietiläinen KH, *et al*. Adverse effects of fructose on cardiometabolic risk factors and hepatic lipid metabolism in subjects with abdominal obesity. Journal of Internal Medicine. 2017; 282: 187–201.
[44] Mirtschink P, Jang C, Arany Z, Krek W. Fructose metabolism, cardiometabolic risk, and the epidemic of coronary artery disease. European Heart Journal. 2018; 39: 2497–2505.
[45] Weisberg SP, McCann D, Desai M, Rosenbaum M, Leibel RL, Ferrante AW. Obesity is associated with macrophage accumulation in adipose tissue. Journal of Clinical Investigation. 2003; 112: 1796–1808.
[46] Ferrante AW Jr. Obesity-induced inflammation: a metabolic dialogue in the language of inflammation. Journal of Internal Medicine. 2007; 262: 408–414.
[47] Zhao H, Raines LN, Huang SC. Carbohydrate and Amino Acid Metabolism as Hallmarks for Innate Immune Cell Activation and Function. Cells. 2020; 9: 562.
[48] Ma EH, Bantug G, Griss T, Condotta S, Johnson RM, Samborska B, *et al*. Serine Is an Essential Metabolite for Effector T Cell Expansion. Cell Metabolism. 2017; 25: 345–357.
[49] Reid MA, Allen AE, Liu S, Liberti MV, Liu P, Liu X, *et al*. Serine synthesis through PHGDH coordinates nucleotide levels by maintaining central carbon metabolism. Nature Communications. 2018; 9: 5442.
[50] Torres C, Alonso CA, Ruiz-Ripa L, León-Sampedro R, Del Campo R, Coque TM. Antimicrobial Resistance in Enterococcus spp. of animal origin. Microbiology spectrum. 2018; 6: 1-41.
[51] Zhang B, Wang X, Xia R, Li C. Gut microbiota in coronary artery disease: a friend or foe? Bioscience Reports. 2020; 40: 1–11.
[52] Merello L, Salazar MR, Elgueta GF, González D, Elton V, Quiroz M, *et al*. Hospital mortality and long-term survival of 103 patients with infective endocarditis requiring surgery. Revista Medica de Chile. 2019; 147: 1535–1542. (In Spanish)
[53] Yang Y, Gao H, Li X, Cao Z, Li M, Liu J, *et al*. Correlation analysis of muscle amino acid deposition and gut microbiota profile of broilers reared at different ambient temperatures. Animal Bioscience. 2021; 34: 93–101.
[54] Liu S, Sun Y, Zhao R, Wang Y, Zhang W, Pang W. Isoleucine increases muscle mass through promoting myogenesis and intramyocellular fat deposition. Food and Function. 2021; 12: 144–153.
[55] Ma Q, Zhou X, Hu L, Chen J, Zhu J, Shan A. Leucine and isoleucine have similar effects on reducing lipid accumulation, improving insulin sensitivity and increasing the browning of WAT in high-fat diet-induced obese mice. Food and Function. 2020; 11: 2279–2290.
[56] Li F, Wang L, Cai Y, Luo Y, Shi X. Safety assessment of desaminotyrosine: Acute, subchronic oral toxicity, and its effects on intestinal microbiota in rats. Toxicology and Applied Pharmacology. 2021; 417: 115464.
[57] Soltani Z, Rasheed K, Kapusta DR, Reisin E. Potential Role of Uric Acid in Metabolic Syndrome, Hypertension, Kidney Injury, and Cardiovascular Diseases: is it Time for Reappraisal? Current Hypertension Reports. 2013; 15: 175–181.
[58] Johnson RJ, Nakagawa T, Jalal D, Sánchez-Lozada LG, Kang DH, Ritz E. Uric acid and chronic kidney disease: which is chasing which? Nephrology Dialysis Transplantation. 2013; 28: 2221–2228.